

Stem Cell Reports, Volume 12

Supplemental Information

**Transient Redirection of SVZ Stem Cells to Oligodendrogenesis by
FGFR3 Activation Promotes Remyelination**

Wenfei Kang, Ken C.Q. Nguyen, and Jean M. Hébert

SUPPLEMENTAL INFORMATION

Supplemental Figures

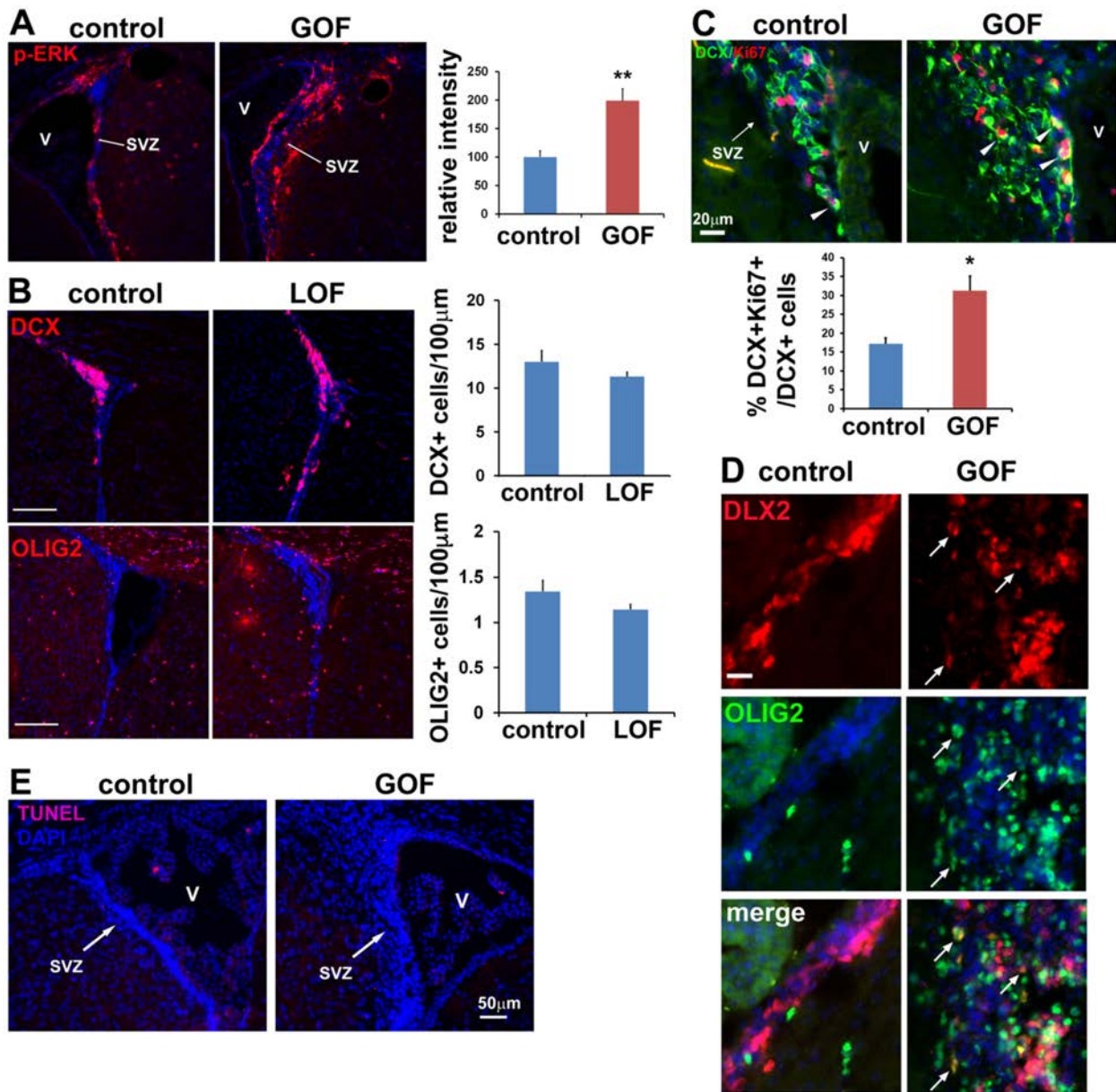


Figure S1. Effects of manipulating FGF receptor activity on p-ERK, neurogenesis, oligodendrogenesis, and apoptosis. Related to Figure 1.

(A) Increased FGFR3 activity leads to an increased level of phospho-ERK, a downstream target of FGF signaling in the SVZ. Immunostaining for p-ERK is significantly brighter in GOF mutants than controls. $p = 0074$.

(B) FGFRs are not required for maintaining apparently normal levels of neurogenesis or oligodendrogenesis in the SVZ. *Nestin-CreER;Fgfr1^{fx/fx};Fgfr2^{fx/fx};Fgfr3^{fx/fx}* (LOF) mice and littermate controls show no difference in DCX or OLIG2 staining. Scale bars, 100 µm.

(C) Increased FGFR3 activity enhances proliferation of neuroblasts. Proliferative neuroblasts in the SVZ are double stained for DCX and Ki67 in both controls and mutants. Quantification shows increased number of double labeled cells in GOF mutants compared to controls ($p = 0.01555$). Arrowheads indicate double labeled cells.

(D) Cells double stained with the neural progenitor marker DLX2 and the OL lineage marker OLIG2 are detected in the SVZ of mutant animals. Arrows indicate double labeled cells. Scale bar: 20 μm .

(E) Increased FGFR3 activity does not influence apoptosis in the SVZ. TUNEL assay shows no difference in the in already very low level of apoptosis between controls and mutants.
V, lateral ventricle.

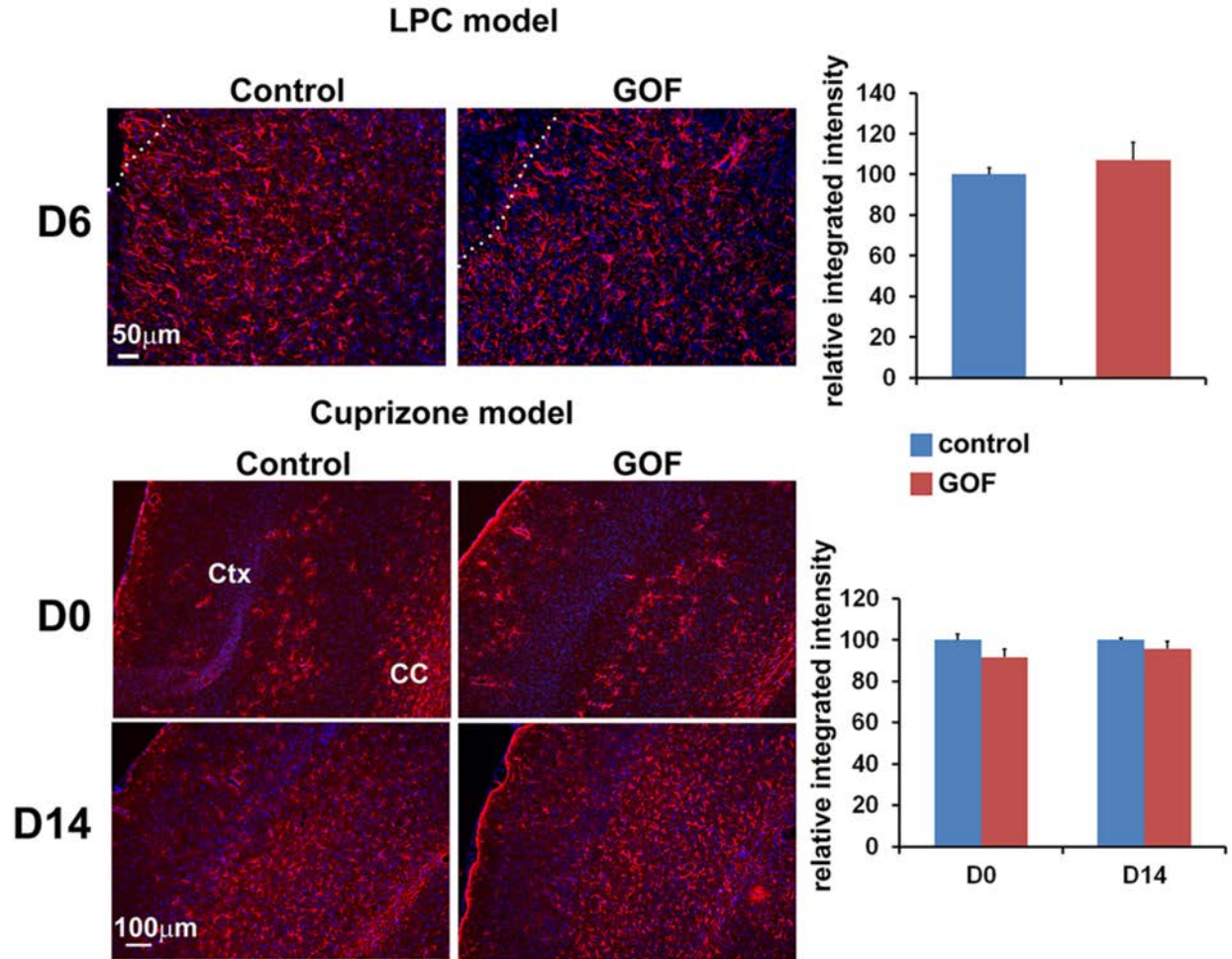


Figure S2. Levels of astrocyte activation in the cortex do not appear enhanced in the GOF mutants after lesioning. Related to Figure 3.

GFAP immunostaining in mutants and controls with LPC- and cuprizone-induced demyelination. Quantification shows comparable relative integrated intensity of GFAP staining in controls and mutants. Dotted lines in images of LPC-induced demyelination indicate the edge of the lesion. Ctx, cortex; CC, corpus callosum.

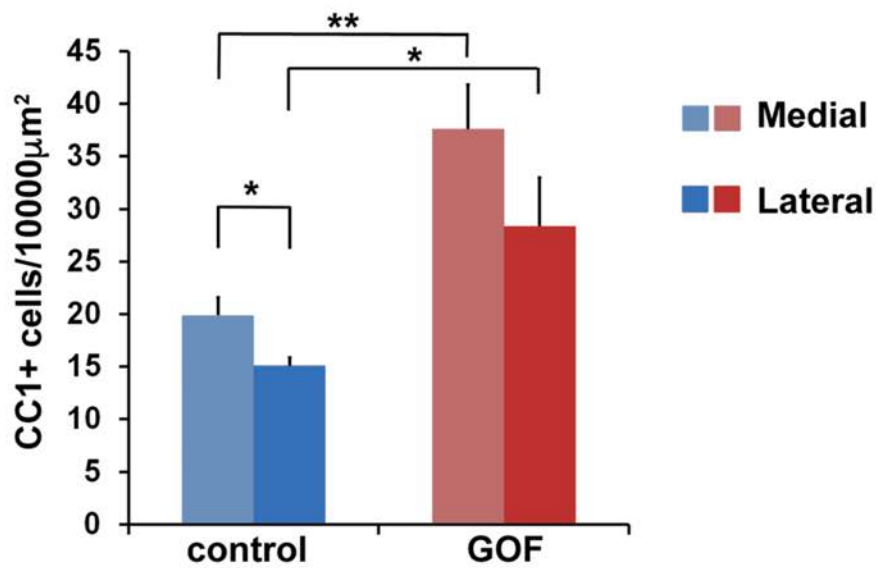
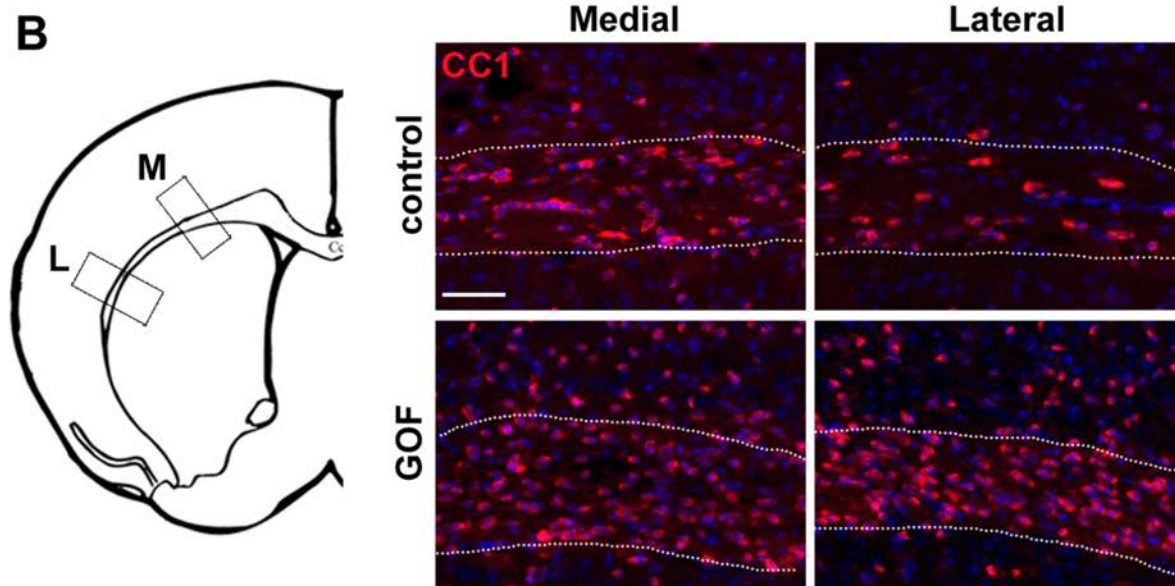
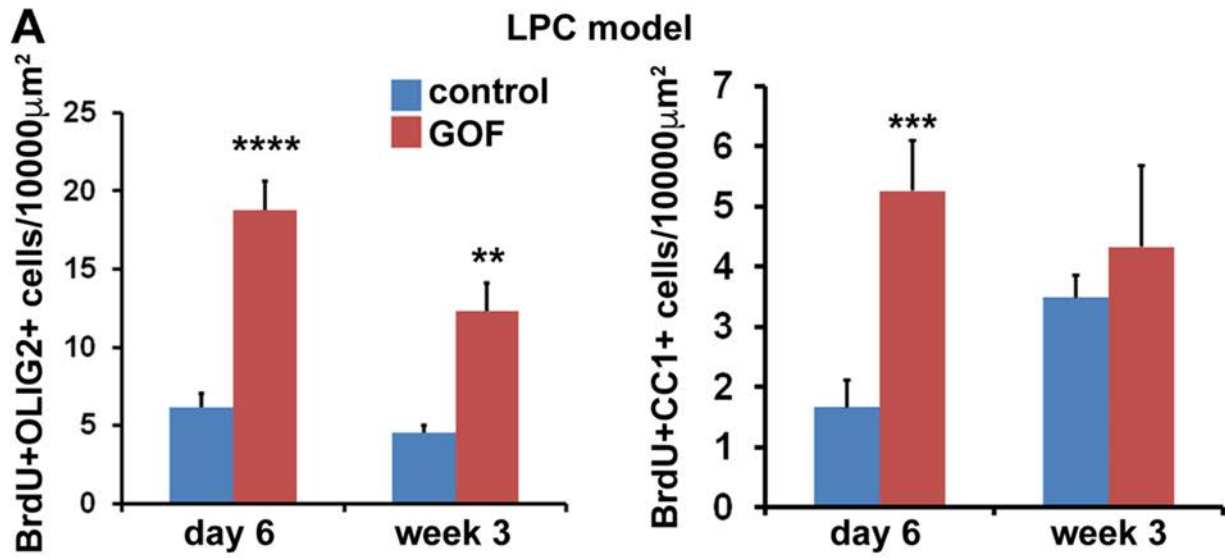


Figure S3. Increased FGFR activity promotes oligodendrocyte regeneration upon LPC-induced demyelination. Related to Figure 4.

(A) Quantification of newly generated oligodendroglial cells labeled by BrdU and OLIG2 and OLs labeled by BrdU and CC1 around the lesion in controls and GOF mutants after LPC-injection indicates a significant increase in the number of both double labeled cells in GOF mutants at 6 days after injection (OLIG2+BrdU+, $p = 7.8 \times 10^{-8}$; CC1+BrdU+, $p = 0.00017$). However, at 3 weeks after injection, although the increase of BrdU+OLIG2 + cells is maintained ($p = 0.0064$), the BrdU+CC1+ cells become comparable in controls and mutants.

(B) GOF mutants exhibit increased recovery of CC1+ cells even in the lateral corpus callosum. OLs labeled by CC1 in medial and lateral corpus callosum in control and mutant animals at 14 days after the stop of cuprizone. Quantification shows that the number of CC1 + OLs in the lateral CC is lower than that in the medial CC in controls, while in GOF mutants, the difference between the two areas is not statistically significant. The corpus callosum is outlined with dotted lines. Position M: medial corpus callosum proximal to the SVZ. Position L: lateral corpus callosum distal to the SVZ. Scale bar: 50 μm . * $p < 0.05$, ** $p < 0.01$.

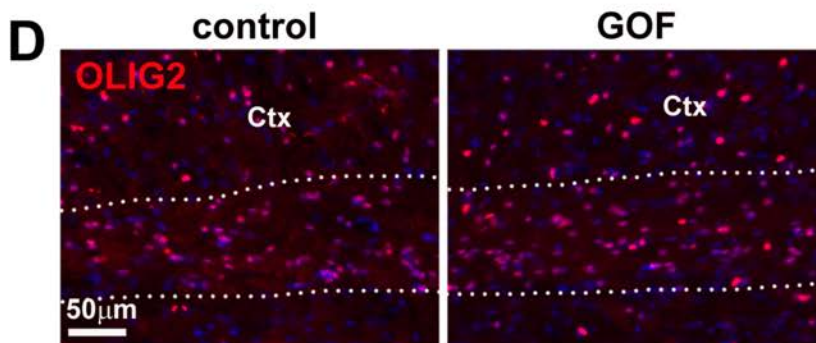
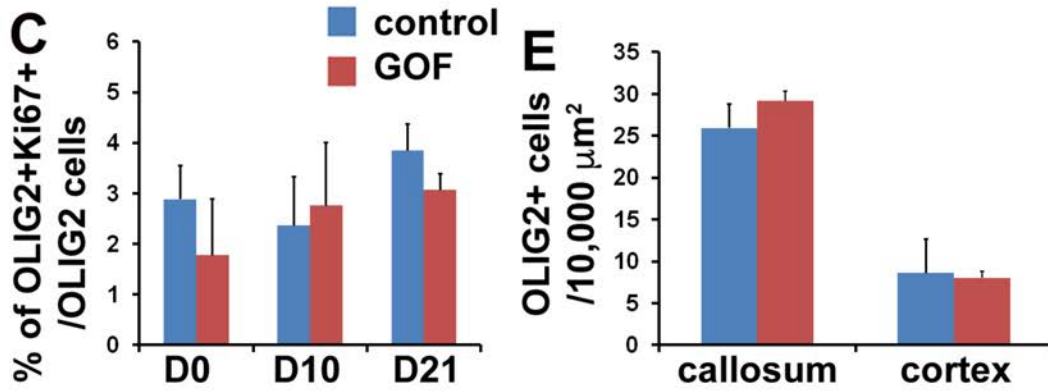
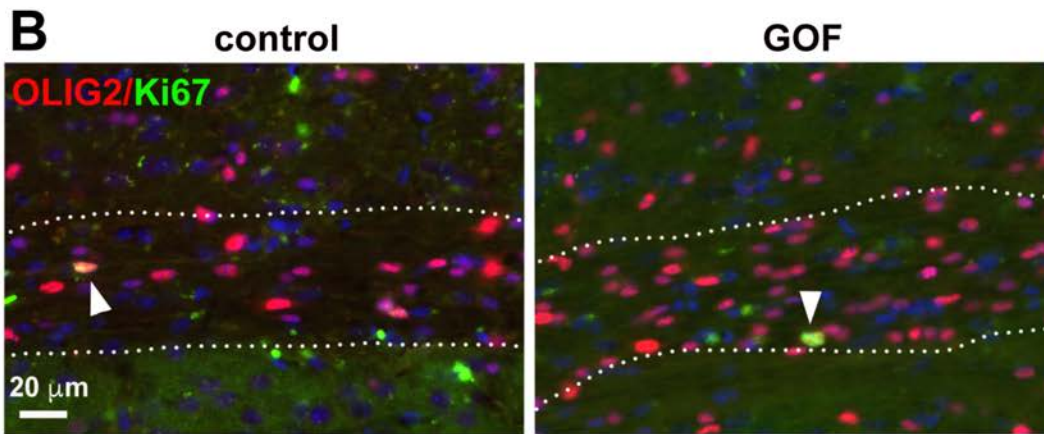
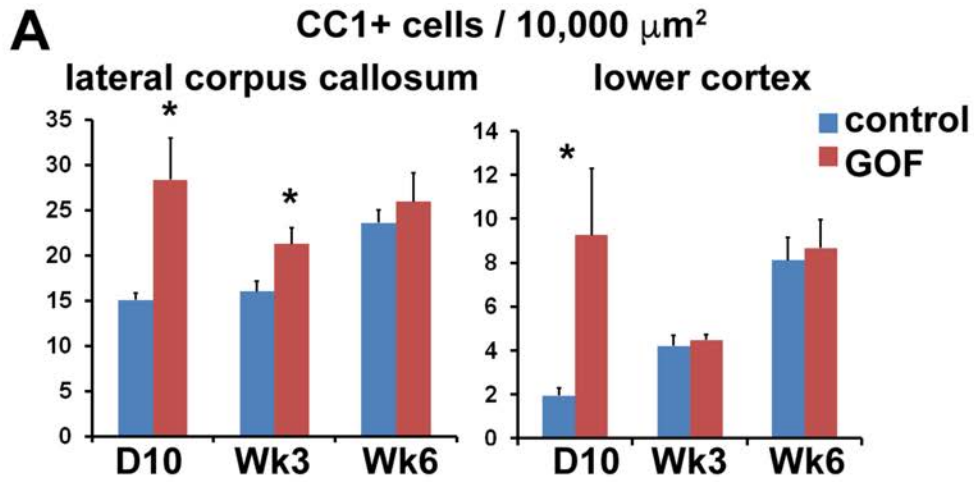


Figure S4. Increased FGFR3 activity promotes OL regeneration upon cuprizone-induced demyelination without affecting parenchymal OPCs. Related to Figure 4.

(A) Quantification of OLs labeled by CC1 in the corpus callosum and lower cortical layers at different time points after cuprizone treatment. Increased numbers of OLs are observed in both the corpus callosum ($p = 0.023$) and lower cortical layers ($p = 0.037$) in GOF mutants at day 10 post cuprizone. The increase is maintained at 3 weeks in the corpus callosum (0.033) but not in the lower cortical layers, while the numbers become comparable at 6 weeks after cuprizone treatment in the corpus callosum and lower layer cortex.

(B) Proliferative pOPCs labeled by OLIG2 and Ki67 in the corpus callosum of controls and mutants at day 10 after cuprizone treatment. The corpus callosum is outlined by dotted lines. Arrowheads indicate double labeled cells.

(C) Quantification of numbers of double labeled cells in the corpus callosum at different time points after cuprizone treatment shows no difference in the proliferative state of pOPCs between controls and mutants.

(D) Oligodendroglial cells labeled by OLIG2 in controls and mutants before cuprizone treatment. Ctx, cortex.

(E) Quantification of OLIG2+ cells shows no difference in the number of oligodendroglia in the corpus callosum and lower cortical layers between controls and mutants before cuprizone treatment.

Supplemental Experimental Procedures

Animals and tamoxifen treatment. The *CAG-flox-stop-flox-Fgfr3TDII*,

Fgfr1^{flox/flox}, *Fgfr2^{flox/flox}*, *Fgfr3^{flox/flox}*, and *Nestin-CreER* mice were described previously (Deng et al., 1996; Trokovic et al., 2003; Yu et al., 2003; Balordi and Fishell, 2007; Su et al., 2010; Kang et al., 2014). All mice used in this study were 2-3 months old at the start of experiments. All mice received Tamoxifen (TM), 20 mg/ml in corn oil, intraperitoneally (5 mg/35 g body weight) every other day for a total of five doses, similar to previously described TM regimens that lead to recombination in ~70% of SVZ NSPCs (Balordi and Fishell, 2007; Kang et al., 2014). Controls used were littermates without *Nestin-CreER*. 3-4 weeks after the last TM dose mice were perfused with 4% paraformaldehyde and brains collected. New cells in the lysolecithin (LPC)-induced demyelination model were labeled with BrdU (100mg/kg body weight) injected intraperitoneally 2X/day for 5 days starting the day after LPC injection.

Demyelination. LPC: 2 μ l of 1% LPC (vol/vol) was injected at “day 0” stereotaxically in the corpus callosum 3-4 weeks after the last dose of TM. At 6 and 14 days post-injection, brains were collected for analysis. Cuprizone: mice were fed 0.2% cuprizone chow for 12 weeks. TM was administered every other day for 5 doses with the last dose given 2 weeks before the end of cuprizone. Brains were collected the day the diet was stopped, or 10 or 21 days later.

Immunostaining. Cryosections (20 microns) on slides were heated in 10 mM sodium citrate, pH 6.0, for antigen retrieval, blocked in normal goat serum, incubated with primary antibodies overnight at 4°C, and with secondary antibodies (AlexaFluor-568 or AlexaFluor-488) (Invitrogen, 1:400) for 1 h at room temperature. Primary antibodies:

rabbit anti-DCX (1:400, Cell Signaling Technology, #4604), guinea pig anti-DCX (1:2000, Millipore, AB2253), mouse anti-DLX2 (1:100, Santa Cruz Biotech. sc393879), rabbit anti-GFAP (1:100, Dako, Z0334) rabbit anti-OLIG2 (1:200 Millipore), rabbit anti-NG2 (1:200, Millipore, AB5320), rabbit anti-CC1 (1:400, Calbiochem, OP80), mouse anti-Neurofilament (1:200, Biolegend, 837901), mouse anti-MBP (1:500, Covance, SMI-99P), rat anti-MBP (1:400, Abcam, ab7349), rat BrdU (1:1000, Bio-Rad, OBT0030G). For staining of BrdU, slides were incubated with 2M HCl at room temperature for 30 min before antigen retrieval. Stained sections were analyzed on a Zeiss AxioSkop2 or a confocal Zeiss LSM-510 MetaDuo V2.

Transmission electron microscopy (TEM). Mice were perfused with phosphate buffer containing 2.5% glutaraldehyde, 2% paraformaldehyde, and 25 mM sucrose (pH 7.2). Brains were postfixed in this solution overnight followed by phosphate buffer washes and vibratome sliced at 800 microns. The corpus callosum was dissected, postfixed with 1% osmium tetroxide, stained with 2% uranyl acetate, dehydrated through an ethanol series, and embedded in resin (LX112, LADD Research Industries, or HardPlus, Electron Microscope Science). Ultrathin sections were cut on a Leica Ultracut UC7 or RMC Powertome XL, stained with 1% uranyl acetate for 10 min, stained with lead citrate, and imaged on a JEOL 1200EX TEM at 80kv. For axon numbers, only axons larger than 0.3 μm were counted.

Quantitation and statistics. Cells were counted in the SVZ or the corpus callosum in coronal sections positionally matched in the rostrocaudal axis for all analyses. For cell counts, the SVZ was defined as the visibly denser layer of DAPI+ nuclei lining the ventricle. Statistical analyses were with the Student's t-test. At least 3 sections per hemisphere for each of 3 mice per genotype were used for cell counts. Numbers were averaged and compared between mutant and control littermates. Data were presented as mean +/-SEM.

Supplemental References

- Balordi F, Fishell G (2007) Mosaic removal of hedgehog signaling in the adult SVZ reveals that the residual wild-type stem cells have a limited capacity for self-renewal. *J Neurosci* 27:14248-14259.
- Deng C, Wynshaw-Boris A, Zhou F, Kuo A, Leder P (1996) Fibroblast growth factor receptor 3 is a negative regulator of bone growth. *Cell* 84:911-921.
- Su N, Sun Q, Li C, Lu X, Qi H, Chen S, Yang J, Du X, Zhao L, He Q, Jin M, Shen Y, Chen D, Chen L (2010) Gain-of-function mutation in FGFR3 in mice leads to decreased bone mass by affecting both osteoblastogenesis and osteoclastogenesis. *Human molecular genetics* 19:1199-1210.

Yu K, Xu J, Liu Z, Sosic D, Shao J, Olson EN, Towler DA, Ornitz DM (2003) Conditional inactivation of FGF receptor 2 reveals an essential role for FGF signaling in the regulation of osteoblast function and bone growth. *Development* 130:3063-3074.